allowing re-functionalization of the freed-up areas with different molecules at will, and the subsequent assembly of colloidal nanoparticles to designed places on top-down fabricated nanoantennas with nanoscale precision. "This scheme allows us to bridge bottom-up synthesis with top-down lithography. I believe this will be a powerful scheme for future parallel nanofabrication," commented Maier.

Maier also showed that hot-electron generation can be used to map sites of optical absorption in metallic nanoclusters with nanoscale precision. Plasmonic antennas with sharp corners showing 'hot spots' for hot-electron injection into molecules — 'chemical hot spots' — were also discussed. "So far, plasmonic nanoparticles have been only investigated for electromagnetic hot spots, but I believe we should embrace the notion of chemical hot spots as well," Maier said.

Miguel Correa-Duarte from the University of Vigo, Spain, gave a talk on the development of hybrid nanostructures to improve the generation of hot electrons in the near-infrared region and their injection into titanium dioxide semiconductor nanocrystals for enhanced performance of photochemical reactions inside living cells. "Hot-electron injection for photocatalysis is advantageous because it allows injection of electrons into a semiconductor nanocatalyst almost in the whole range of the visible and infrared, and improves the catalytic performance of the catalysts. The challenge is to better understand the hot-electron injection mechanism and to clearly distinguish it from thermal catalysis," said Correa-Duarte.

In recent years, a growing number of studies have also been devoted to the interaction of plasmonic nanostructures with ultrashort laser pulses. The precise determination of the amount of energy absorbed by the metal nanostructures at each pulse is essential to optimize applications in ultrafast photonics. By properly modelling the ultrafast energy exchanges during the interaction of a plasmonic nano-object and ultrashort light pulses, Bruno Palpant from the University of Paris Saclay, France, showed that the optical absorption efficiency of the interactions evolved on the pulse timescale due to the multiphotonic generation of a strongly out-of-equilibrium hot-electron distribution. "The challenge is to rule out any morphological pulse-induced change to retain only pure electronic nonlinearities in the response measured. The amount of energy absorbed definitely has to be calibrated by accounting for the effect of hot electrons," said Palpant.

Since hot electrons decay very fast, on the femtosecond to picosecond timescale, ultrafast spectroscopy is crucial to understand and optimize their behaviour. Transient absorption allows the energy redistribution processes in plasmonic nanostructures following light absorption to be followed in detail and visualized in real time.

Giulio Cerullo from the Polytechnic University of Milan, Italy, reviewed all the ultrafast relaxation processes following light absorption by plasmonic nanostructures, from the very early electron–electron relaxation processes, occurring on the 100-fs timescale and forming a thermalized electron distribution, which could be resolved using transient absorption spectroscopy with 10-fs time resolution, through to electron–phonon scattering on the picosecond timescale, to, finally, energy re-equilibration of the nanostructure with the surroundings. He showed that transient absorption allows sensitive detection of the mechanical vibrations of nanostructures. However, he also pointed out that the limitation of current transient absorption experiments is that they are typically performed on ensembles of nanostructures, thus averaging over their inhomogeneous properties. This detection mode washes away many effects that sensitively depend on the exact shape of the nanostructure and thus vary from one to the next.

"Experiments on single plasmonic nanostructures using transient absorption microscopy will be highly beneficial and should be developed more in the future. Also, experiments with high temporal resolution, down to 10 fs, will be crucial in order to capture the non-thermalized hot-electron distribution. Finally, studies of hybrid plasmonic nanostructures, such as metal–semiconductor or metal–molecule hybrids, especially in the strong-coupling regime between excitonic and plasmonic resonances, will be very interesting because of the rich underlying physics and the important applications," Cerullo said.

The field of hot electrons in plasmonic nanostructures is undoubtedly promising, yet there is still much to do. The challenges are, as summarized by Govorov, to better understand the hot-electron mechanisms, to distinguish between hot-electron photochemistry and thermal photochemistry, to increase energy efficiencies for chemical reactions and for hot-electron photodetectors, and to find important reactions where the hot-electron effect can be beneficial. Furthermore, it is important to better understand the interactions of hot electrons with ultrashort laser pulses and to monitor the hot-electron distributions on single plasmonic nanostructures at high temporal resolution.

The next NanoPlasm conference will return to Cetraro, Italy, from 15–19 June 2020. ❐

Rachel Won
Nature Photonics, *London, UK.*
e-mail: r.won@nature.com

Published online: 27 July 2018
https://doi.org/10.1038/s41566-018-0226-0

OPTICAL COMMUNICATIONS

Integrated combs drive extreme data rates

A chip-based optical frequency comb source has now been successfully used to send 661 Tbit s^{-1} over 9.6 km of multicore fibre, bringing considerable savings in the energy consumption and size of data transmission equipment.

Daniel J. Blumenthal

In the early 1970s, one of the world's first commercial fibre-optic links was turned on in Chicago, running at 45 Mbit s^{-1}. It was thought at the time that the transmission bandwidth problem was solved. Now, writing in *Nature Photonics*, a team of researchers from Denmark and Japan reports the demonstration of a chip-based optical comb source capable

of transmitting an astounding 661 Tbit s^{-1} in 2,400 channels over an optical fibre containing 30 cores[1]. This capacity is roughly equivalent to the amount of data flowing through the worldwide Internet daily traffic[2].

The Internet continues to drive fibre optic transmission to unprecedented bandwidths due to the explosive growth of video and the Internet of Things. New solutions are needed to mitigate the increased power demands of the Internet communications infrastructure that today represents almost 10% of the world's energy consumption[2]. The use of traditional, discrete lasers to drive global data flows are running into complexity and power limitations as fibre transmission rates explode. The chip-based comb generator reported by Hu and colleagues serves as a single multi-frequency optical source with the fidelity to transmit at these extreme data rates and demonstrates a record-breaking 66% power conversion efficiency[1].

A single strand of fibre can carry upwards of 20 Tbit s^{-1} (ref. [3]) with laboratory records pushing 65 Tbit s^{-1} (ref. [4]). To achieve this transmission capacity, wavelength-division multiplexing (WDM) is employed, where a large array of lasers operating at distinct wavelengths are used to pack parallel data streams onto a single fibre. To push WDM capacity, complex electrical and optical modulation techniques are applied to each wavelength using a combination of time, frequency and phase, along with sophisticated pulse and spectral shaping, and digital signal processing techniques[5] often implemented in specialized digital signal processors (DSPs).

These techniques can be pushed until transmission rates come up against the well-known Shannon limit . To scale beyond this limit, researchers create additional physical lanes using polarization-division multiplexing (PDM), with data transmitted on separate polarization states, spatial-division multiplexing (SDM)[6], where multiple light-carrying cores are fabricated within a fibre, and mode-division multiplexing (MDM), where multiple spatial modes are transmitted on each core[7].

Capacity is scaled even further using optical 'superchannels'[5] where data is modulated and multiplexed onto tightly packed Nyquist frequency channnels and across overlapped frequencies, fibre cores and spatial modes using powerful techniques such as forward error correction (FEC) and digital signal processors running multiple-input–multiple-output (MIMO) algorithms[8]. It is conceivable that in the near future, undersea cables will carry tens of petabits of data per second, yet scaling to these capacities using today's discrete WDM optical source solutions will run into severe energy-efficiency, complexity, cost and stability issues.

As a result, compact optical frequency comb generators (a single source that simultaneously emits multiple regularly spaced wavelengths) are being investigated as an alternative to ever larger arrays of discrete WDM lasers. An optical frequency comb source that is coherently modulated in time, frequency and phase, and parallel multiplexed or bundled into a superchannel using WDM, PDM, SDM and MDM is illustrated in Fig. 1.

So-called 'hero transmission experiments' based on frequency comb sources built from discrete components have already set record transmission capacities, notably 2.15 Pbit s^{-1} transmission over a 22-core fibre with 6.468 Tbit s^{-1} superchannels coded on 399 individual 25-GHz-spaced frequencies in the C and L bands in the 1,500–1,600 nm telecoms window[9]. Moving these systems to chip-scale integrated sources with the view to creating compact, energy-efficient Tbit s^{-1} transceivers is the next big challenge. For this to be feasible, integrated comb lasers must deliver comparable performance to their discrete component counterparts, including a large channel count, equal and sufficient power in each line, sufficiently low noise and precise telecom frequency spacing across the transmission bandwidth (typically 10–100 GHz channel spacing, over ~4 THz for the C band).

Compact comb designs include the use of mode-locked lasers (MLLs)[10], high-speed phase modulators[11], gain-switched comb sources[12], and microresonator Kerr frequency combs[13,14]. Of these, Kerr microresonator combs have the advantage of a wide comb spacing (>100 GHz) for high baud rate modulation that is difficult to achieve with other comb techniques, extremely uniform mode spacing, high stability and sufficient output power and optical signal-to-noise ratio (OSNR) to enable high-capacity coherent transmission. In particular, the dissipative Kerr soliton microresonator comb generator[15] addresses key stability and noise issues. These devices use a balance of nonlinear four-wave mixing parametric gain, cavity loss, dispersion and nonlinearity to generate continuously circulating pulses in an optical microresonator that yield a stable frequency comb output.

It should be noted that MLLs combined with subsequent nonlinear phase-shift-induced spectral broadening in a dispersive medium with the correct dispersion sign (anomalous dispersion), leads to compression of the mode-locked pulses. This compression is balanced with frequency chirping that occurs during spectral broadening, producing a coherent broadened optical comb[16] and is the technique used by Hu and colleagues[1]. In this process, newly generated frequencies at the leading edge of the pulse travel slower than the newly generated frequencies at the pulse trailing edge, leading to continual spectral broadening and pulse compression, akin to soliton pulse propagation in the time domain and cascaded four-wave mixing in the frequency domain.

Hu and colleagues report a world record transmission capacity of 661 Tbit s^{-1} using a single optical comb source over 9.6 km of single-mode 30-core fibre[1]. The comb source is a two-stage design incorporating a 5-mm-long nonlinear aluminium-gallium-arsenide-on-insulator (AlGaAsOI) nanowaveguide pumped by a stable MLL comb. The AlGaAsOI nanowaveguide generates a total of 400 coherent 10-GHz-spaced frequencies (40-kHz linewidth) via the self-phase modulation (SPM) optical nonlinear effect and is pumped by a 10-GHz MLL driven by a low-noise radio-frequency (RF) oscillator. Hu et al. report an astonishing 66% conversion efficiency, almost two orders of magnitude higher than Kerr microresonator combs that have ~1% conversion efficiency. The researchers model the system, finding an overall 20–25% power consumption saving over using equivalent discrete laser transmitters to build a 661 Tbit s^{-1} link. Using a single-pass waveguide, Hu and co-workers demonstrate comb generation that is temperature insensitive from 20–34 °C, providing energy savings over the temperature stabilization and feedback and locking control circuits that are required for resonator-based approaches.

While this is not the first demonstration of a chip-based optical comb frequency source for coherent WDM communications[17,18], the achievement of a transmission capacity approaching 1 Pbit s^{-1} is an important milestone. In Hu and colleagues' work, the link capacity is initially set by the quality of the MLL pump laser, with a pulse repetition rate and frequency spacing set by the RF clock oscillator that was measured to be at Hz level frequency stability. Stable MLL operation is determined by the spectral purity of the RF drive source without requiring active feedback[19]. While not reported in the work of Hu et al., it is straightforward to further lock the MLL output to a standardized telecommunications frequency reference.

This combination of accuracy and stability are key to extreme data rate transmission. To keep optical losses

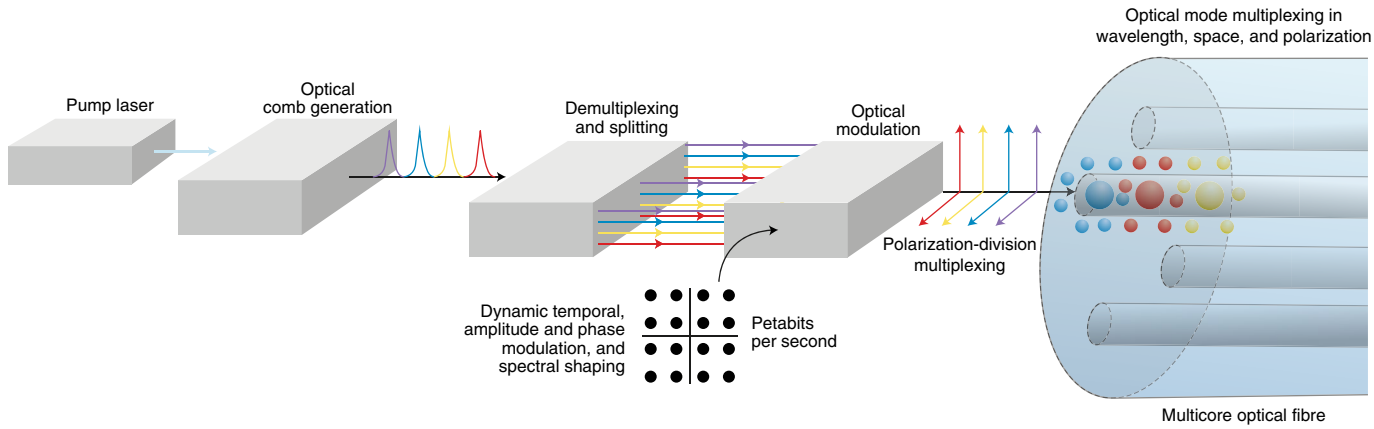

Fig. 1 | Generating extreme transmission data rates with a single chip-scale optical frequency comb source. An optical frequency comb generator is coherently modulated by terabits of data channels in time, frequency and phase, and parallel multiplexed or bundled into a superchannel on a multicore optical fibre using WDM, PDM, SDM and MDM techniques.

manageable, propagation losses in the AlGaAsOI nanowaveguide are reduced by careful control of the surface quality of the waveguide's top, bottom and side walls. The resulting 0.75-dB loss is impressive as is the nonlinear figure of merit of 660 W^{-1} m^{-1}. The device is designed so that waveguide dispersion dominates material dispersion and enables operation in the anomalous group velocity dispersion regime of the full 1,550 nm C-band to balance chirp and pulse compression.

The result is a compact, high stability, high OSNR, low linewidth comb source capable of transmitting 2,400 coherent modulated PDM parallel data channels on 80 wavelengths in each of 30 SDM fibre cores. The original comb is generated with a 10-GHz RF oscillator with 1-Hz frequency stability driving and a MLL that produces coherent 80 × 10 GHz spaced channels in ~6.4 nm optical bandwidth. This comb is subsequently broadened in the AlGaAsOI nanowaveguide to 400 × 10 GHz channels in ~44 nm optical bandwidth. In Hu and colleagues' experiment, every 5th of the 400 comb frequency lines are filtered after data modulation to produce a grid of 80 × 50 GHz spaced data channels that have the stability of the original 10-GHz master oscillator. The 50-GHz spacing is required to support the final transmitted bandwidth of 40 gigabaud (GBd) per wavelength with an additional 10-GHz guard band. This portion of the experiment resulted in useful converted optical frequencies being discarded, effectively lowering the overall energy efficiency, and could be recovered by using a 50-GHz MLL with equivalent frequency stability performance.

Hu and colleagues use six physical degrees of freedom to modulate and multiplex data: amplitude, phase, frequency, time, polarization and space. First, the researchers prepared the comb source spectrum to produce a uniform −11 dBm per comb line at the input to the data modulator, limited by the maximum modulator input power for all 400 comb lines. The energy used to produce new comb lines via SPM in the passive AlGaAsOI nanowaveguide depletes the original comb frequencies as shown in Fig. 2 of ref. [1]. A multichannel programmable wavelength-selective switch (WSS) is used to seamlessly reinsert a tapped version of the original MLL spectrum back into the SPM generated comb and is made possible by the coherence and stability of the nanowaveguide output spectrum relative to the MLL pump spectrum. The final 80 comb lines are equalized before modulation while maintaining a high OSNR for each channel as shown in Fig. 4b of ref. [1]. Three erbium-doped fibre amplifier stages are employed to compensate for optical losses in the system.

The transmission channel capacity was built up through a series of modulation and multiplexing techniques. As with most transmission experiments of this magnitude, a single optical data modulator is used, and data in the individual channels must be decorrelated before transmission using time delays to simulate independent data streams. Hu and colleagues accomplish this by first modulating random data onto the 10 Gbit s^{-1} 400 frequency comb generator pulses using a single 16-QAM optical coherent modulator where each pulse occupies a quarter of a 10 Gbit s^{-1} time slot. This modulation generates a 16-point symbol constellation in the in-phase (I) and quadrature (Q) space. Each point, or symbol in this space represents a unique combination of 4 bits at a 10-GBd rate. The coherent encoded data stream is split into 4 optical copies, each delayed by integer multiples of a bit-interval to decorrelate the data and recombined to create an optical time-division multiplexed 40-GBd 16-QAM data stream. This encoded 40 GBd × 4 bits Bd^{-1} data stream on 400 optical frequency channels is split into two orthogonal PDM states, with one arm delayed to further decorrelate data between polarization states, to generate 40 GBd × 4 bits Bd^{-1} × 2 PDM = 320 Gbit s^{-1} per each of the 400 wavelengths. This parallel 400 × 10 GHz spaced wavelength stream is input to a second WSS that separates it into even and odd channels as well as performing a rectangular 40-GHz passband filter function, matched to the baud rate, on a 50-GHz frequency grid. The rectangular passbands allow even tighter packing density of the 40-GBd 16-QAM channels, generating Nyquist-filtered pulses in the time domain. These pulses are centred in each time slot and overlap into neighbouring time slots with the pulse energy zeros purposely located at the centre of neighbouring time slots to minimize intersymbol interference between adjacent time slots.

The output even and odd channels are passed through independent optical delays to further decorrelate the neighbouring channel data to simulate fully loaded independent data transmission channels. At this point in the transmission system, 80 × 320 Gbit s^{-1} channels on a 50-GHz frequency grid are combined using a third WSS and power split and amplified to produce 30 copies of 16-QAM modulated WDM/TDM/PDM 25.6 Tbit s^{-1} channels. The 30 spatial 25.6 Tbit s^{-1} data streams are further delayed and decorrelated before being connected

to a 30-core optical fibre using a fibre-to-waveguide 3D spatial multiplexer.

The 30-core fibre employs a design with four different fibre cores types and arrangement that keeps the crosstalk between adjacent cores below –50 dB and is able to transmit 30×25.6 Tbit $s^{-1} = 768$ Tbit s^{-1} over a distance of 9.6 km without the need for MIMO processing. The researchers assumed this capacity represented data coded with FEC, a technique used to allow error-free end-to-end data recovery in the presence of transmission errors. FEC is achieved by redundantly coding bits, and two widely used approaches are soft-decision FEC (SD-FEC) that requires ~20% transmission overhead (the precise number varies depending on the technique) and hard-decision FEC (HD-FEC) that requires 7% transmission overhead. Hu and colleagues measured each channel independently using a 3D spatial fibre demultiplexer to a waveguide fan-out. A coherent receiver that detects each polarization using a polarization diversity optical 90° hybrid circuit is connected to each of the 30 fan-out ports one at a time. The 90° hybrid is also coupled to a tunable laser local oscillator that is tuned to each of the 80 wavelengths one at a time, for coherent recovery of 4-level eye diagrams on balanced photodetectors.

These waveforms are digitally collected and processed offline using digital signal processing techniques to perform steps needed to estimate the bit error rate (BER) including carrier recovery, phase estimation, channel filtering, phase lock loop, threshold decision and BER determination. The researchers report a post-FEC error-free data recovery of 10^{-15} BER. After the coherent receiver and offline digital signal processing, 58 WDM channels were measured to perform better than the SD-FEC threshold and 22 channels better than the HD-FEC threshold. When the overhead is subtracted for the number of channels reaching each threshold, an error-free transmission capacity of 661 Tbit s^{-1} is calculated.

This work is an important step towards realizing compact, energy- and cost-efficient terabit and petabit transceivers and fibre optic links that scale with future Internet traffic capacity. The integration of comb generators with the pump laser and other transceiver components including multiplexing and demultiplexing components, spectral shaping, optical amplifiers, optical isolators, and arrays of coherent modulation and demodulation and receiver elements is an important next step.

Looking to the future, utilizing a higher repetition rate MLL with a Hz-level stability RF clock source will allow all comb lines to be utilized. The number of frequencies in Hu and colleagues' work requires a commensurate number of data modulators and receivers, in this case 2,400, leading to other energy-efficiency issues that include power-hungry modulator drivers and receiver transimpedance amplifiers. In the future, systems will operate at the emerging 64 GBd rate and later at higher baud rates as well using higher-order QAM modulation formats (for example, 256-QAM), reducing the number of modulators and receivers. Integration of the AlGaAs material with a silicon or silicon nitride platform poses issues related to the integration technology and packaging. Future generations of extreme capacity links will benefit from approaches such as that reported by Hu and colleagues to efficiently keep up with the exploding capacity of the Internet and its global energy consumption. ❐

Daniel J. Blumenthal
Department of Electrical and Computer Engineering, University of California, Santa Barbara, CA, USA.
e-mail: danb@ucsb.edu

Published online: 27 July 2018
https://doi.org/10.1038/s41566-018-0222-4

References

1. Hu, H. et al. *Nat. Photon.* https://doi.org/10.1038/s41566-018-0205-5 (2018).
2. *Cisco Visual Networking Index: Forecast and Methodology, 2016–2021* White Paper No. 1465272001663118 (Cisco, 2018).
3. Cai, J.-X. et al. 20 Tbit/s capacity transmission over 6,860 km. In *Optical Fiber Communication Conference/National Fiber Optic Engineers Conference 2011* PDPB4 (OSA, 2011).
4. Ghazisaeidi, A. et al. 65Tb/s transoceanic transmission using probabilistically-shaped PDM-64QAM. In *ECOC 2016-Post Deadline Paper; 42nd European Conference on Optical Communication* 1–3 (2016).
5. Winzer, P. J. *Opt. Photon. News* **26**, 28–35 (2015).
6. Richardson, D. J., Fini, J. M. & Nelson, L. E. *Nat. Photon.* **7**, 354–362 (2013).
7. van Uden, R. G. H. et al. *Nat. Photon.* **8**, 865–870 (2014).
8. Liu, X., Chandrasekhar, S. & Winzer, P. J. *IEEE Signal Process. Mag.* **31**, 16–24 (2014).
9. Puttnam, B. J. et al. 2.15 Pb/s transmission using a 22 core homogeneous single-mode multi-core fiber and wideband optical comb. In *2015 European Conference on Optical Communication* 1–3 (2015).
10. Wang, Z. et al. *Light Sci. Appl.* **6**, e16260 (2017).
11. Weimann, C. et al. *Opt. Express* **22**, 3629–3637 (2014).
12. Pfeifle, J. et al. *Opt. Express* **23**, 724–738 (2015).
13. Del'Haye, P. et al. *Nature* **450**, 1214–1217 (2007).
14. Kippenberg, T. J., Holzwarth, R. & Diddams, S. A. *Science* **332**, 555–559 (2011).
15. Herr, T. et al. *Nat. Photon.* **8**, 145–152 (2014).
16. Roelkens, G. et al. Frequency comb generation in III-V-on-silicon photonic integrated circuits. In *Advanced Photonics 2016* (IPR, NOMA, Sensors, Networks, SPPCom, SOF) OSA technical Digest (online) paper IM2A.5 (OSA, 2016).
17. Levy, J. S. et al. *Nat. Photon.* **4**, 37–40 (2010).
18. Brasch, V. et al. *Science* **351**, 357–360 (2016).
19. Quinlan, F. et al. *Opt. Lett.* **31**, 2870–2872 (2006).